AD-A173 996 INTERPRETATION OF ELECTROSTATIC NOISE OBSERVED BY VOYAGER 1 IN TITAN'S WAKE(U) IOWA UNIV IOWA CITY DEPT OF PHYSICS AND ASTRONOMY T Z MA ET AL. JUN 86 1/1

UNCLASSIFIED U. OF IOWA-86-26 N00014-85-K-0404 F/G 3/2 NL

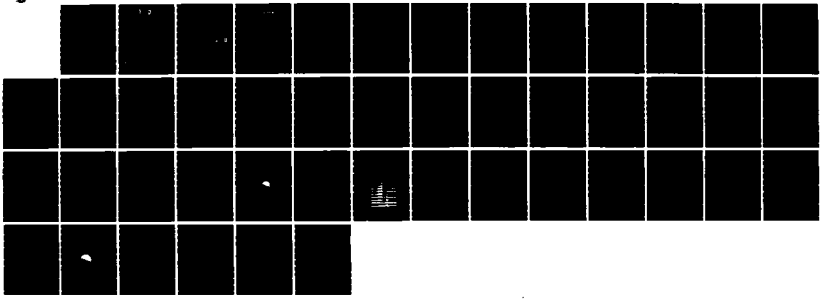

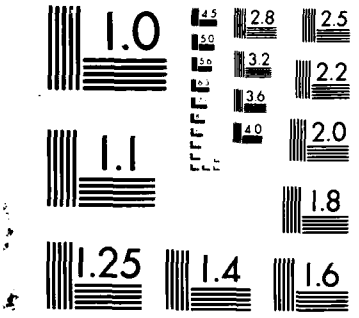

INTERPRETATION OF ELECTROSTATIC NOISE OBSERVED BY VOYAGER 1 IN TITAN'S WAKE

by

T. Z. Ma and D. A. Gurnett

Department of Physics and Astronomy

THE UNIVERSITY OF IOWA

Iowa City, Iowa 52242

(12)

U. of Iowa 86-26

INTERPRETATION OF ELECTROSTATIC NOISE OBSERVED BY VOYAGER 1 IN TITAN'S WAKE

by

T. Z. Ma and D. A. Gurnett

June 1986

Submitted to J. Geophys. Res.

Department of Physics and Astronomy
The University of Iowa
Iowa City, IA 52242

UNCLASSIFIED

SECURITY CLASSIFICATION OF THIS PAGE (When Data Entered)

REPORT DOCUMENTATION PAGE	READ INSTRUCTIONS BEFORE COMPLETING FORM
1. REPORT NUMBER: U. of Iowa 86-26	2. GOVT ACCESSION NO.: AD-A173 996
	3. RECIPIENT'S CATALOG NUMBER:
4. TITLE (and Subtitle): Interpretation of Electrostatic Noise Observed by Voyager 1 in Titan's Wake	5. TYPE OF REPORT & PERIOD COVERED: Progress June 1986
	6. PERFORMING ORG. REPORT NUMBER:
7. AUTHOR(s): T. Z. Ma and D. A. Gurnett	8. CONTRACT OR GRANT NUMBER(s): N00014-85-K-0404
9. PERFORMING ORGANIZATION NAME AND ADDRESS: Dept. of Physics and Astronomy, The University of Iowa, Iowa City, IA 52242	10. PROGRAM ELEMENT, PROJECT, TASK AREA & WORK UNIT NUMBERS:
11. CONTROLLING OFFICE NAME AND ADDRESS: Electronics Program Office, Office of Naval Research, Arlington, VA 22217	12. REPORT DATE: 12 July 1986
	13. NUMBER OF PAGES: 42
14. MONITORING AGENCY NAME & ADDRESS(if different from Controlling Office)	15. SECURITY CLASS. (of this report): UNCLASSIFIED
	15a. DECLASSIFICATION/DOWNGRADING SCHEDULE:

16. DISTRIBUTION STATEMENT (of this Report)

Approved for public release; distribution is unlimited.

17. DISTRIBUTION STATEMENT (of the abstract entered in Block 20, if different from Report)

18. SUPPLEMENTARY NOTES

19. KEY WORDS (Continue on reverse side if necessary and identify by block number)

Electrostatic Noise
Titan
Voyager 1
Ion Beam Plasma Interactions

20. ABSTRACT (Continue on reverse side if necessary and identify by block number)

(See following page)

DD FORM 1 JAN 73 1473 EDITION OF 1 NOV 65 IS OBSOLETE
S/N 0102-LF-014-6601

UNCLASSIFIED

SECURITY CLASSIFICATION OF THIS PAGE (When Data Entered)

ABSTRACT

During the Voyager 1 spacecraft flyby of Titan on November 12, 1980, an intense broadband low frequency electric field noise was observed in the inbound wake. This so-called sheath noise is believed to be generated by an ion beam-plasma interaction between the ions in the corotational Saturnian magnetospheric plasma and nearly stationary plasma created by the ionization of Titan's atmosphere. The analysis is based on the information from Voyager 1 and reasonable assumptions. The results agree quite well with the observation. The analysis shows that the instability only occurs where the density of the corotational ions is comparable to the density of ions originating from Titan's atmosphere. The growth rate is high enough to generate the observed noise, and the calculated and observed frequency ranges are in good agreement.

I. INTRODUCTION

During the Voyager 1 spacecraft flyby of Saturn's moon, Titan, on November 12, 1980, the plasma wave instrument detected various kinds of plasma wave emissions. There were upper hybrid resonance emissions, radio emissions from Saturn and a broad band of low frequency electric field noise [Gurnett et al., 1981; 1982]. The purpose of this paper is to investigate the origin of the low frequency electric field noise.

Titan is the only moon in the solar system known to have a substantial atmosphere. At the time of the Voyager 1 flyby, Titan was located within the outer magnetosphere of Saturn. It has been found that Titan has no appreciable intrinsic magnetic field. Therefore, its atmosphere interacts directly with the magnetosphere of Saturn [Ness et al., 1981]. Hartle et al. [1982] described a model of this interaction, which is shown in Figure 1. The Voyager 1 trajectory, projected into the Saturnian equatorial plane, is indicated by the line labeled V1 trajectory near the bottom of the diagram. The electric field noise occurs in the cross-hatched region from about 0532:30 to 0538:30 Spacecraft-Event-Time (SCET). This noise was called sheath noise by Gurnett et al., because it is qualitatively similar to the electrostatic wave seen in the magnetosheath at Earth and in the ionosheath at Venus [Gurnett et al., 1982; Rodriguez, 1979; Scarf et al., 1980]. A similar kind of noise was also observed near the upstream

edge of the ionized gas clouds produced by the AMPTE (Active Magnetospheric Plasma Tracer Explorers) solar wind ion releases [Gurnett et al., 1985; 1986]. In these cases, the origin of the noise was explained by an ion beam-plasma interaction between the nearly stationary ions produced by the gas cloud and the rapidly flowing solar wind protons.

In the present case, the sheath noise is believed to be generated by an ion beam-plasma interaction between the corotational Saturnian magnetospheric plasma and the nearly stationary plasma created by ionization of Titan's atmosphere. In Section II of this paper we will summarize the observations related to the wave phenomena and a detailed analysis will be made in Section III.

II. SUMMARY OF OBSERVATIONS

The properties of magnetospheric plasma just outside of the wake region are fundamental to the magnetospheric interaction with Titan's atmosphere. It has been known from the Voyager 1 experiments that there are at least two major components, H^+ and N^+, in the magnetosphere near the orbit of Titan. In addition, N_2^+ and H_2CN^+ were also possibly present [Hartle et al., 1982]. Neubauer et al. [1984] summarized the basic properties of the magnetospheric plasma near the orbit of Titan. The number density of protons was about 0.1 cm^{-3}, and of nitrogen ions, N^+, was about 0.2 cm^{-3}. The other possible components were minor and will be ignored in the analysis of this paper. The temperatures of H^+ and N^+ ions were 210 eV and 2.9 keV, respectively. The electron number density and temperature were about 0.3 cm^{-3} and 200 eV. To a good approximation the plasma flow velocity was in the corotational direction (20° deflected toward Saturn). The speed ranged from about 80 to 150 km/s, somewhat less than the corotational speed near Titan's orbit, which is 200 km/s.

Titan's exosphere has been studied in detail by Hartle et al. [1982]. The major composition in the exosphere is molecular nitrogen, N_2, and atomic hydrogen, H. The densities of N_2 and H were observed to be 10^8 cm^{-3} and 4×10^4 cm^{-3} at the exobase, which is 4000 km from the center of Titan (see Figure 1) [Broadfoot et al., 1981]. Assuming a temperature of 160°K, Hartle et al. [1982] derived the radial density

distributions shown in Figure 2. The density scale height of N_2 was about 150 km, and that of H was about 1500 km.

The upper hybrid resonance emissions observed in the vicinity of Titan provided a plasma density profile along the trajectory of the spacecraft. The top panel of Figure 3 shows the plasma density profile. This figure was reproduced from Gurnett et al. [1982]. The inbound sheath, the tail region and outbound sheath, if there is one, were marked. The density level of magnetospheric plasma, N^+ and H^+, which was about 0.3 cm^{-3}, is indicated by the dashed line. As can be seen in the figure, the density was enhanced up to 40 cm^{-3} in the vicinity of Titan. Since the plasma in the wake originated mostly from the photoionization of exospheric particles, the plasma density profile was basically governed by the exosphere density distribution. The scale height of the plasma density is about 500 km, which indicates that the densities of H and N_2 must be comparable in this region. However, there is no information about the fractions of H^+ and N^+, or any other minor species, such as N_2^+ or H_2CN^+.

The low frequency electric field intensities detected by the plasma wave spectrum analyzer are shown in the bottom panel of Figure 3. The sheath noise from 0532:30 to 0538:30 SCET, is clearly distinguishable from the noise in the tail region, from 0539:30 to 0545:30 SCET. The sheath noise has a broad frequency range, from 10 to 1000 Hz. A representative spectrum of this noise, at the point marked by an arrow in Figure 3, is shown in Figure 4. The spectrum has a broad peak centered at a frequency of about 100 to 200 Hz. The broadband electric

field strength is about 0.5 mVm^{-1}. As can be seen from Figure 3, the frequency of the sheath noise has a tendency to increase as the spacecraft approached Titan. During this time the plasma density increased monotonically along the trajectory. However, a clear cutoff is seen at about 0539:00 SCET, when the density is about 15 cm^{-3} to 20 cm^{-3}. The intense noise was only observed on the inbound leg, which is on the dayside of Titan, and was essentially absent on the outbound leg, which is on the nightside.

III. ORIGIN OF THE SHEATH NOISE

The plasma processes in the wake region are known to be complicated and involve ionization, mass loading, and ion acceleration. To try to understand the origin of the plasma wave noise, a simple model will be used. Since the sheath noise occurred at the region where the corotational magnetospheric plasma flow streams through the nearly stationary plasma from Titan's exosphere, an ion-beam plasma instability is a likely candidate to generate the noise. A reduced (one-dimensional) velocity distribution for the model is qualitatively shown in Figure 5. Six groups of particles are considered: cold and hot electrons, magnetospheric N^+ and H^+, and exospheric N^+ and H^+ from Titan. Minor constituents are neglected. In the assumed model, each component is represented by a drifting Maxwellian velocity distribution. The drift velocity of the magnetospheric N^+ and H^+ is the magnetospheric flow velocity, V_m, which is taken to be 150 km/sec. The drift velocity of the exospheric N^+ and H^+ is approximately zero. Because the electron cyclotron radius is small, both the cold and hot electrons drift at the $\vec{E} \times \vec{B}$ drift velocity, V_d. Since there is no information about the drift velocity of electrons, we assume that the electrons drift in such a way that the total current is zero. The validity of this assumption can be verified by estimating the possible current density from the variation of the magnetic field over the interaction region. The magnetic field varies about 4 nT over 4 Titan radii. Therefore, the current density is not more

than 3×10^{-10} A/m^2. Taking the particle number density to be .3 cm^{-3}, it can be shown that the shift induced in the relative velocity between the electrons and ions is only 7 km/sec, which is less than 10%. The current essentially does not affect our instability analysis. Before one can proceed with an instability analysis, assumptions must be made concerning several parameters that are either not well known or were not measured.

First, the electron temperature in the interaction region is not completely known. Most likely the electron temperature is similar to that in the magnetosphere, except there must be a cold component associated with the photoionization of exospheric neutral particles. Therefore, we assume that there are two groups of electrons, hot and cold. The hot electrons are assumed to have a temperature, T_e^h, of 200 eV, which is the temperature of the magnetospheric plasma. The cold electrons are assumed to have a temperature, T_e^c, from 2 eV to 200 eV. The lower limit is the temperature that would result from photoionization by the ultraviolet light and the upper limit takes into account the possible heating of the photoelectrons up to magnetospheric temperatures. Finally, the temperature of the exospheric N^+ and H^+ is unknown. This temperature is presumably close to the exosphere temperature, which is about 186°K. The electron drift velocity, V_d, is determined by the current $\vec{J} = \sum_i n_i e_i \vec{V}_i = e[N_b \vec{V}_m - (N_b + N_s)\vec{V}_d]$, where N_b and N_s are defined in Table 1. Assuming $\vec{J} = 0$, one obtains

$$V_d = \frac{N_b V_m}{N_b + N_s} \quad . \tag{1}$$

A summary of all parameters and their assumed values is given in Table 1.

A summary of all parameters and their assumed values is given in Table 1.

Instabilities associated with an ion beam-plasma interaction were first analyzed by Fried and Wong [1966]. An ion beam-plasma interaction was proposed by Gurnett et al. [1985] to interpret the low frequency electrostatic noise observed in an AMPTE solar wind lithium release. Similarly, it can be applied here. For a multispecies unmagnetized plasma the electrostatic instability is determined by the reduced distribution function,

$$F(v) = \sum_s \frac{m_e}{m_s} F_s(v) \quad , \qquad (2)$$

where m_s and $F_s(v)$ are the mass and distribution function of s^{th} species, and m_e the electron mass. The summation is over all species. The plasma is unstable when F(v) is sufficiently double-humped to satisfy the penrose criterion [Krall and Trivelpiece, 1973]. As can be seen from Figure 5, instabilities are in principle possible for phase velocities between 0 and V_d and between V_d and V_m. However, the thermal velocity of the beam ions is about equal to V_m, which is larger than V_m-V_d. Therefore, the instability between V_d and V_m cannot occur because the beam ion distribution is too broad to produce a double hump. Instability can only occur in association with the relatively cold exospheric ions at phase velocities between 0 and V_d.

Before proceeding with the analysis we will consider the effect of the magnetic field. In the present problem, the magnetic field is essentially perpendicular to the plane of Titan's orbit and therefore to

the plasma flow direction. Its magnitude is about 5 nT. The electron cyclotron frequency is about 140 Hz. The cyclotron frequency of a proton is less than 0.1 Hz and that of an N^+ ion is even less. The wave frequency we consider here is much larger than the ion cyclotron frequency. Therefore the effect of the magnetic field on the ion motions is negligible. The electron cyclotron frequency is almost in the middle of the wave frequency range. In general, electrons should be treated to be magnetized. However, the gyroradius of the thermal electron is 9.5 km [Neubauer, 1984]. Even for the photoelectrons, the gyroradius is an order of km. It is anticipated that the wavelength of the electrostatic noise will be short, probably only several tens of meters. For such short wavelengths, much less than the cyclotron radius, the wave motion is basically not affected by the magnetic field. The theoretical proof for this result was given by K. N. Stepanov [1959]. Therefore, we will neglect the magnetic field in the calculation and verify the consistency afterwards. Another effect of the magnetic field is that it could affect the distribution functions of the exospheric N^+ and H^+ ions, which may differ from our assumption. We will discuss this effect later.

The linearized electrostatic wave dispersion relation for a multispecies plasma with no magnetic field is given by

$$D(k,\omega) = 1 - \sum_s \frac{\omega_s^2}{k^2} \int \frac{\partial F_s/\partial v}{v - \omega/k}\, dv = 0 \qquad (3)$$

where k is the projection of wave number on the beam direction, ω is the complex frequency whose real part gives the frequency and imaginary

part gives the growth rate for the instability, and ω_s is the plasma frequency for s^{th} species. If $F_s(v)$ is a Maxwellian distribution, the dispersion equation (3) can be written as

$$D(k,\omega) = 1 - \frac{1}{2} \sum_s \frac{1}{(k\lambda_{Ds})^2} Z'(z_s) \approx 0 \qquad (4)$$

where λ_{Ds} is the Debye length for s^{th} species, Z' denotes the derivative of the plasma dispersion function (see Fried and Conte [1961] with respect to its argument, and z_s is

$$z_s = (\frac{\omega}{k} - V_s)/a_s \qquad (5)$$

where a_s, V_s are the thermal and drift velocity of s^{th} species, respectively. The dispersion equation is solved numerically by using Salzer's method to evaluate the plasma dispersion function and Muller's method for root-finding [Fried and Conte, 1961; Salzer, 1951; Muller, 1956].

Figure 6 shows a representative growth rate for the ion-beam plasma instability. The top panel shows the wave number, k, normalized by the Debye length, λ_D, as a function of frequency. The bottom panel shows the growth rate, γ, vs. frequency. The parameters used here are as follows: $N_{ps} = N_{ns}$, $N_s = 5 \times N_b = 1.5$ cm^{-3}, $T_e^c = 200$ eV, i.e., $N_e^c = 0$, $N_e^h = N_s + N_b$, and the values of the parameters in Table I are also used. With the above parameters, the Debye length is computed to be about 0.77m. Taking $k\lambda_D$ to be 0.05 or higher, the wavelength is

estimated to be about 20m or less. This wavelength is consistent with the assumption that the magnetic field can be neglected. As seen in Figure 6, the growth rate is very high, up to 6 sec^{-1}, which means that a wave disturbance can grow a thousand times larger in 1 second. At Voyager 1's closest approach, the radial distance to the center of Titan was about 6500 km. As is shown in Figure 1, the unstable region in the upstream side of the spacecraft path has the scale size of at least 6500 km. The wave encountered by the spacecraft must start in this region, and propagates downstream along with the plasma flow. If a wave starts 1000 km upstream of the spacecraft path, for example, it takes 5 seconds (at a speed of 200 km/sec, including the wave propagation) to reach the spacecraft. During this time the wave can grow to 10^{15} times, which is more than enough to grow from a thermal level to very high amplitudes. The frequency range, up to 200 Hz, agrees very well with the spectrum in Figure 4.

For the calculations in Figure 6, the wavevector, $\vec{k}$, is parallel to the beam velocity. It can be shown that for the assumed parameters a wave propagating parallel to the beam velocity has the highest growth rate. Figure 7 gives the maximum growth rate, γ_{max}, (maximized over $|\vec{k}|$) as a function of θ, the angle between $\vec{k}$ and $\vec{V}_m$ under the condition of $N_{ps} = N_{ns}$, $N_s = N_b$. The solid curve is for the case of no cold electrons, and the dashed curve is for the case $N_e^c = N_s$. As can be seen in the figure, the growth rates for both cases decrease monotonically as θ increases, and the instabilities cease at about 85°. Similar results are obtained in the variety of the conditions in Table 1. Therefore,

in the rest of the study we will consider the most unstable case, that is, $\theta = 0$.

In order to study the effect of the plasma density on the instability, the marginal instability condition ($\gamma = 0$) must be investigated as a function of the plasma-beam density ratio, N_s/N_b. Figures 8 and 9 show the frequency of marginal instability as a function of density ratio, N_s/N_b. The dashed curves in these plots show the frequencies corresponding to the maximum growth rates. Figures 10 and 11 show the maximum growth rate versus N_s/N_b. The conditions for Figures 8 and 10 are that $N_{ns} = N_{ps}$, $T_e^c = T_e^h = 200$ eV, $N_e^c = 0$, and $N_e^h = N_s + N_b$. The conditions for Figures 9 and 11 are that $N_{ns} = N_{ps}$, $T_e^h = 200$ eV, $T_e^c = 2$ eV, $N_e^c = N_s$, and $N_e^h = N_b$. The parameters not mentioned take the values given in Table 1. These two groups of figures cover the two extreme limits for the electron temperatures. The two extremes give very similar results. As can be seen in Figures 10 and 11, the maximum growth rates reach about 10 sec^{-1}, which is quite high. The frequency range extends up to several hundred Hz, which is in good agreement with the observed frequency range. One of the most important features in Figures 8 and 9 is that the instability only occurs for a limited range of density ratio, N_s/N_b, between about 0.001 to 50 for $n_e^c = 0$, and between about 0.001 to 25 for $N_e^c = N_s$. This condition shows that the instability cannot occur too far from Titan, where the newly created plasma density is too low or too close to Titan where the newly created plasma density is too high. This result explains the region where the noise occurs in Figure 3. As can be seen, the sheath noise started about six minutes before Voyager 1's closest approach to Titan where

the density ratio is much less than 1, and it ceased at the place where the density ratio is about 50, in good agreement with the theory. As mentioned in Section II, the frequency range increased as the density increased. Figures 8 and 9 predict this same trend. The unstable frequencies start from a few Hz when the density ratio is about 10^{-3} and increase monotonically to a few hundred Hz as the density ratio increases to about 50. The effect of the different fractions of N^+ and H^+ on the instability has been studied. The results are similar to Figures 8 -11 except that more protons give a slightly larger frequency range.

No sheath noise was observed in the outbound wake. There are two reasons for this inbound-outbound asymmetry. One is a day-night asymmetry. The outbound wake is on the nightside. There is less photoionization on the outbound wake than in the inbound wake, which is on the dayside. The other is the direction of acceleration of the newly created ions. This is shown in Figure 12. On the inbound side of Titan, the ions are accelerated away from the exosphere and therefore can escape downstream. The free escape caused the density enhancement. However, on the outbound side of Titan, the ions are accelerated into the exosphere and are absorbed (see Gurnett et al. [1982] and Bridge et al. [1981]).

In the above analysis, we have assumed that every species of particles has a Maxwellian velocity distribution. This is certainly a good assumption in the absence of a static field. However, in the present case, there is a magnetic field, which is roughly perpendicular to

the Titan's equatorial plane, and an electric field, which is induced by the corotational motion of the Saturnian magnetosphere. Therefore, the validity of this assumption should be discussed for each species.

As is shown in the upper panel of Figure 13, if a constant $\vec{B}$ field is in -z direction and an $\vec{E}$ field is in x direction, then the charged particles will gyrate in the x-y plane in addition to the drift motion in y direction. In the case of a homogeneous plasma, the velocity distribution in the x-y plane will be a ring with the radius of V_o, which is equal to cE/B, as shown in the lower panel of Figure 13. However, if the temperature of a particle is high, such that the thermal velocity, V_{th}, is greater than V_o, the distribution function will be close to a single Maxwellian. In the present problem, the thermal velocities of electrons are about 850 km/sec (for T_e^c = 2 eV) to 8500 km/sec (for T_e^h = 200 eV). The thermal velocities of the beam H^+ and N^+ are about 200 km/sec. They are greater than V_o, which is taken to be 150 km/sec. Therefore, for these four species, the Maxwellian distribution is a good assumption. Since the exospheric H^+ and N^+ have very low temperatures, their thermal velocities are only a few km/sec, which is much less than V_o. Therefore, the effect of the magnetic field on the distribution of these two species must be considered in detail.

A ring distribution in the x-y plane can be modeled by a function as

$$f(v_x, v_y, v_z) = f_1(v_z) f_2(v_x, v_y) \qquad (6)$$

where $f_1(v_z)$ is just a single Maxwellian and

$$f_2(v_x, v_y) = \frac{1}{2\pi^{3/2} V_o a} \exp\left[-\left(\sqrt{v_x^2 + (v_y - V_o)^2} - V_o\right)^2/a^2\right] \qquad (7)$$

where $a = \sqrt{2kT/m}$, and T, m is the temperature and the mass of the particle, respectively. A plot of $f_2(v_x, v_y)$ is shown in the lower panel of Figure 13. By taking $f_2(v_x, v_y)$ to be the distribution function for the exospheric H^+ and N^+, we find that the ion beam-plasma instability is stabilized.

To explain this, in Figure 14 we plot the one-dimensional distribution function $F(v) = \int f_2(V_x, V)\, dV_x$ for protons with temperature T = 186°K and V_o = 150 km/sec. The subscript y is dropped in the one-dimensional function. The plot shows F(v) for v between -5 km/sec to 150 km/sec because of the symmetry of F(v) about v = V. This plot is very different from a single Maxwellian distribution with the same temperature and V_o = 0 in the following sense. Firstly, the peak of the present distribution function near v = 0 is much lower than the peak of the single Maxwellian because the particles for the latter are mostly concentrated in an interval of less than 10 km/sec, about v = 0, while less than 10% of particles for the former stay in the same interval. Secondly, for the single Maxwellian, the distribution function is almost zero for v > 10 km/sec, while for F(v) in Figure 14, there is tail-like distribution with finite negative slope except at v = 150 km/sec. Because of this factor, no positive slope is obtained

when we introduce an ion beam with a temperature of 210 eV and drift velocity of 150 km/sec, and electrons with temperatures more than 2 eV and drift velocity $0 < V_D < 150$ km/sec. Therefore the ion beam-plasma instability cannot occur in this situation.

In doing this calculation, a homogeneous plasma is assumed. This assumption is valid if the scale length of the interaction region, L, is much larger than the particle gyroradius, R_c. In the present case, the scale length is about 500 km to 2000 km. The lower limit is obtained from the measured plasma density profile shown in Figure 3, and the upper limit is basically the scale length of hydrogen radial distribution for Titan's exosphere (see Figure 2). The gyroradius of the newly created exospheric H^+ and N^+ are 248 km and 3470 km, respectively. From these estimates we see that the ion gyroradii, R_e, is comparable to the scale length of the interaction region, L. The formation of a ring distribution requires that nearly the same number of particles move in every direction. Apparently, this requirement is not met because a large number of particles would go out of the region before completing one gyration. Also, the electric field acting on the newly created ions is not as large as $|\vec{V}_o \times \vec{B}|$ because of the shielding effect of the electrons. From these facts we believe that the newly created ions dominate with the velocity nearly zero, and that a single Maxwellian distribution is still a good assumption.

IV. CONCLUSION

The low frequency electric field noise observed by Voyager 1 during the inbound crossing of Titan's wake has been analyzed in detail. The analysis shows that the noise is generated by an ion beam-plasma instability caused by the corotational magnetospheric ions, mostly H^+ and N^+, streaming through the nearly stationary plasma produced by photoionization of Titan's exosphere. This mechanism explains the basic features of the noise. By using known (measured) and reasonably-assumed parameters, one gets high growth rates, and good agreement with the observed frequency range. The instability has a limited range for the plasma to beam density ratio, N_s/N_b, from about 0.001 to 50. This explains why the noise only occurs in the inbound wake.

However, some detailed aspects of the noise cannot be explained because of the lack of some information and the complication of the process in the Titan-magnetospheric interaction. For instance, the calculated frequency for the maximum growth rate does not match the observations in detail, and also, the calculated frequency range for the particular density ratio does not follow observed density exactly. Actually, the detailed process in the interaction region is not well known. Also, for sufficiently high growth rates, nonlinear effects are always present. Nonlinear effects stabilize the system, saturate the wave growth and broaden the frequency spectrum. Therefore, a simple

linear theory is not expected to explain the sheath noise completely. Plasma simulations are required to fully investigate nonlinear effects, including the role of these waves in heating the plasma.

A similar kind of noise was also observed in the vicinity of the space shuttle [Shawhan and Murphy, 1983], apparently caused by an interaction of gases from the shuttle with the surrounding ionosphere. This type of noise seems to be a common phenomena when a neutral gas interacts with a rapidly moving plasma.

ACKNOWLEDGEMENTS

This research was supported by NASA through grant NGL-16-001-043 with NASA Headquarters and contract 954013 with the Jet Propulsion Laboratory, and by the Office of Naval Research through contract N00014-85-K-0404.

REFERENCES

Bridge, H. S., J. W. Belcher, A. J. Lazarus, S. Olbert, J. D. Sullivan, F. Bagenal, P. R. Gazis, R. E. Hartle, K. W. Ogilvie, J. D. Scudder, E. C. Sittler, A. Eviatar, G. L. Siscoe, C. K. Goertz, and V. M. Vasyliunas, Plasma observations near Saturn: Initial results from Voyager 1, Science, 212, 217, 1981.

Broadfoot, A. L., B. R. Sandel, D. E. Shemansky, J. B. Holberg, G. R. Smith, D. F. Strobel, J. C. McConnell, S. Kumar, D. M. Hunten, S. K. Atreka, T. M. Donahue, H. W. Moos, J. L. Bertaux, J. E. Blamont, R. B. Pomphrey, and S. Linick, Extreme ultraviolet observations from Voyager 1 encounter with Saturn, Science, 212, 206, 1981.

Fried, B. D., and S. D. Conte, The Plasma Dispersion Function, Academic Press, New York, 1961.

Fried, B. D., and A. Y. Wong, Stability limits for long longitudinal waves in ion beam-plasma interactions, Phys. Fluids, 9, 1084, 1986.

Gurnett, D. A., W. S. Kurth, and F. L. Scarf, Plasma waves near Saturn: Initial results from Voyager 1, Science, 212, 239, 1981.

Gurnett, D. A., F. L. Scarf, and W. S. Kurth, The structure of Titan's wake from plasma wave observations, J. Geophys. Res., 87, 1395, 1982.

Gurnett, D. A., R. R. Anderson, B. Häusler, G. Haerendel, O. H. Bauer, R. A. Treumann, H. C. Koons, R. H. Holzworth and H. Lühr, Plasma waves associated with the AMPTE artificial comet, Geophys. Res. Lett., 12, 851, 1985.

Gurnett, D. A., T. Z. Ma, R. R. Anderson, O. H. Bauer, G. Haerendel, B. Häusler, G. Paschmann, R. A. Treumann, H. C. Koons, R. Holzworth, and H. Lühr, Analysis and interpretation of the shock-like electrostatic noise observed during the AMPTE solar wind lithium releases, J. Geophys. Res., 91, 1301, 1986.

Hartle, R. E., E. C. Sittler, Jr., K. W. Ogilvie, J. D. Scudder, A. J. Lazarus, and S. K. Atreya, Titan's ion exosphere observed from Voyager 1, J. Geophys. Res., 87, 1383, 1982.

Krall, N. A., and A. W. Trivelpiece, Principles of Plasma Physics, McGraw-Hill, N. York, 473, 1973.

Muller, D. E., A method for solving algebraic equations using an automatic computer, Math. Comp., 10, 208, 1956.

Ness, N. F., M. H . Acuña, R. P. Lepping, J. E. P. Connerney, K. W. Behannon, L. F. Burlaga and F. M. Neubauer, Magnetic field studies by Voyager 1: Preliminary results at Saturn, Science, 212, 211, 1981.

Neubauer, F. M., D. A. Gurnett, J. D. Scudder, and R. E. Hartle, Titan's magnetospheric interaction, Saturn, The University of Arizona Press, 760-781, 1984.

Rodriguez, P., Magnetosheath electrostatic turbulence, J. Geophys. Res., 84, 917, 1979.

Salzer, H. E., Formulas for calculating the error function of a complex variable, Math. Tables, p. 67, 1951.

Scarf, F. L., W. W. L. Taylor, C. T. Russell, and R. C. Elphic, Pioneer Venus plasma wave observations: The solar wind-Venus interaction, J. Geophys. Res., 85, 7599, 1980.

Shawhan, S. D., and G. B. Murphy, Plasma diagnostics package assessment of the STS-3 orbiter environment, J. Spacecraft and Rockets, Special STS-3/OSS-1 issue, 1983.

Stepanov, K. N., Low-frequency oscillations of a plasma in a magnetic field, Soviet Physics JETP, 35(8), 808, 1959.

TABLE 1.

Quantities	Notations	Values
H^+ density in beam	N_{pb}	0.1 cm^{-3}
N^+ density in beam	N_{nb}	0.2 cm^{-3}
Total density in beam	N_b (= N_{pb} + N_{nb})	0.3 cm^{-3}
Newly created H^+ density	N_{ps}	Variable
Newly created N^+ density	N_{ns}	Variable
Total newly created density	N_s (= N_{ps} + N_{ns})	Variable
H^+ temperature in beam	T_{pb}	210 eV
N^+ temperature in beam	T_{nb}	2.9 keV
Exospheric H^+ temperature	T_{ps}	186°K
Exospheric N^+ temperature	T_{ns}	186°K
Hot electron temperature	T_e^h	200 eV
Cold electron temperature	T_e^c	2 eV ~ 200 eV
Beam velocity	V_m	150 km/sec
Electron drift velocity	V_d	Variable
Cold electron density	N_e^c	Variable
Hot electron density	N_e^h	Variable

FIGURE CAPTIONS

Figure 1 The magnetospheric plasma flow around Titan and Voyager 1 trajectory, projected in the Saturnian equatorial plane. The electrostatic noise was observed in the cross-hatched region. Since this noise occurs in a sheath-like region around Titan, it is called sheath noise.

Figure 2 The radial density distribution of Titan's exosphere, normalized by the density of H at the exobase, n_o [Hartle et al., 1982].

Figure 3 The electron density profile along the Voyager 1 trajectory provided by UHR emissions (top panel) and the low frequency electric field noise observed in the vicinity of Titan. The dashed line in the top panel indicates the total density of the magnetospheric plasma. The sheath noise appeared from 0532:30 to 0538:30 SCET, and tail noise appeared from 0539:30 to 0545:30 SCET.

Figure 4 The electric field spectral density of the sheath noise at the time marked by the arrow in Figure 3.

Figure 5 A model for analyzing an ion beam-plasma instability. The magnetospheric H^+ and N^+ ions flow with speed V_m, and electrons (hot and cold) drift with speed V_d, the newly created ions are nearly stationary. The curves are not drawn to scale.

Figure 6 Plots of the growth rate, γ, and normalized wave number, k, as a function of frequency under the conditions $N_s = 5\ N_b = 1.5\ cm^{-3}$, $N_{ns} = N_{ps}$, and $N_e^c = 0$.

Figure 7 The maximum growth rates as a function of θ, and the angle between $\vec{k}$ and $\vec{V}_m$ under the conditions $N_{ns} = N_{ps}$ and $N_s = N_b$. The solid curve is for the case $N_e^c = 0$, and the dashed curve is for $N_e^c = N_s$.

Figure 8 The frequency of marginal stability, r = 0, as a function of the density ratio, N_s/N_b, assuming $N_{ns} = N_{ps}$, and $N_e^c = 0$. The dashed curve indicates the frequency associated with the maximum growth rate.

Figure 9 The same plot as in Figure 8 with $N_e^c = N_s$ and $T_e^c =$ 2 eV.

Figure 10 The maximum growth rate as a function of the density ratio, N_s/N_b, for the case in Figure 8.

Figure 11 The maximum growth rate as a function of the density ratio, N_s/N_b, for the case in Figure 9.

Figure 12 An illustration of representative ion trajectories in the sheath. Ions escape from the exosphere on the inbound side and are absorbed by the exosphere on the outbound side.

Figure 13 Upper panel: If $\vec{B} = -B_o\hat{z}$ and $\vec{E} = E_o\vec{x}$, then the ions gyrate in the x-y plane with velocity $V_o\hat{y}$. L and R_c indicate the scale length and gyroradius, respectively. Lower panel: A ring distribution forms if $L >> R_c$ and the thermal velocity is much less than the drift velocity.

Figure 14 Reduced one-dimensional distribution function for a ring distribution of protons with temperature of 186°K and drift velocity V_o = 150 km/sec. In the interval of velocity from 5 km/sec to 150 km/sec, this tail-like distribution has a finite negative slope.

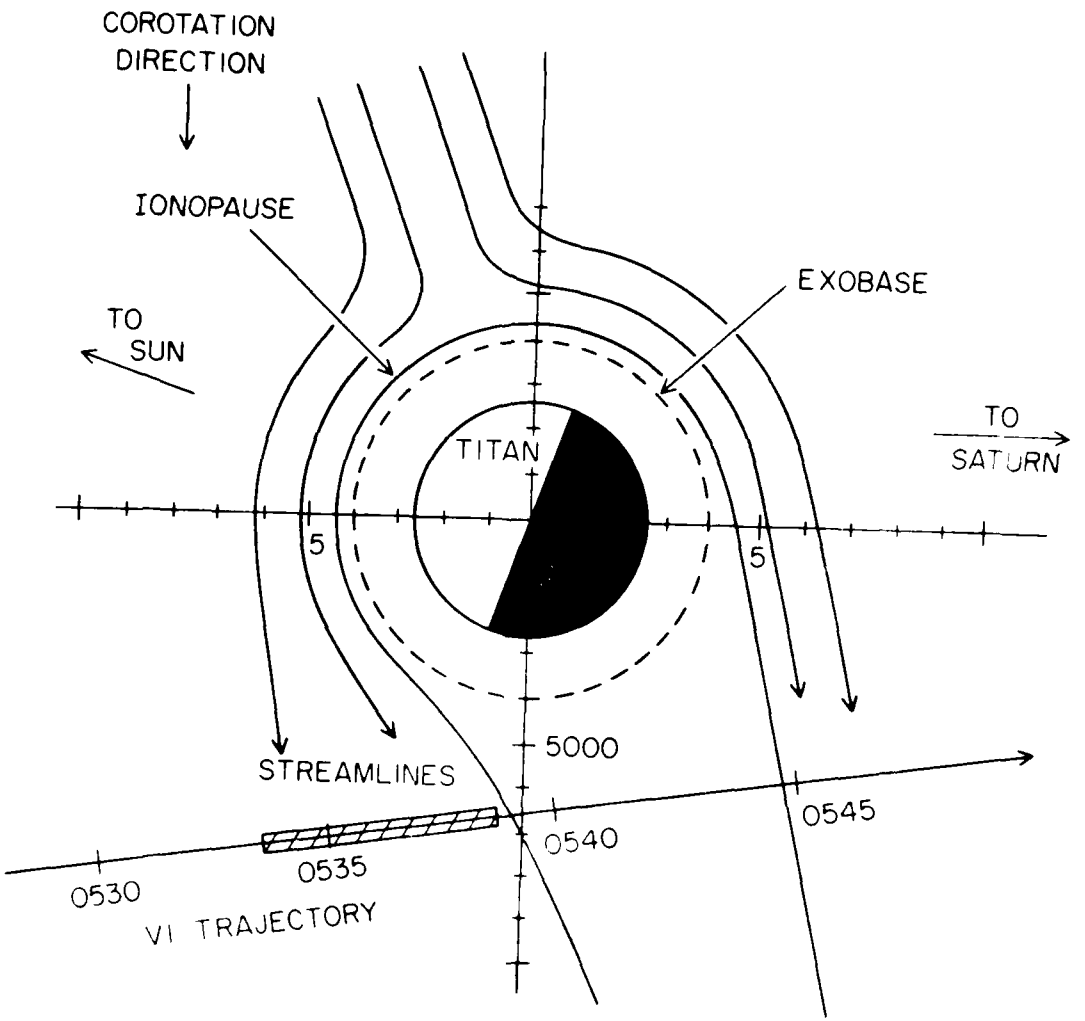
COROTATION
DIRECTION
IONOPAUSE
EXOBASE
TO
SUN
TO
SATURN
TITAN
5
5
5000
STREAMLINES
0530
0535
0540
0545
VI TRAJECTORY

Figure 1

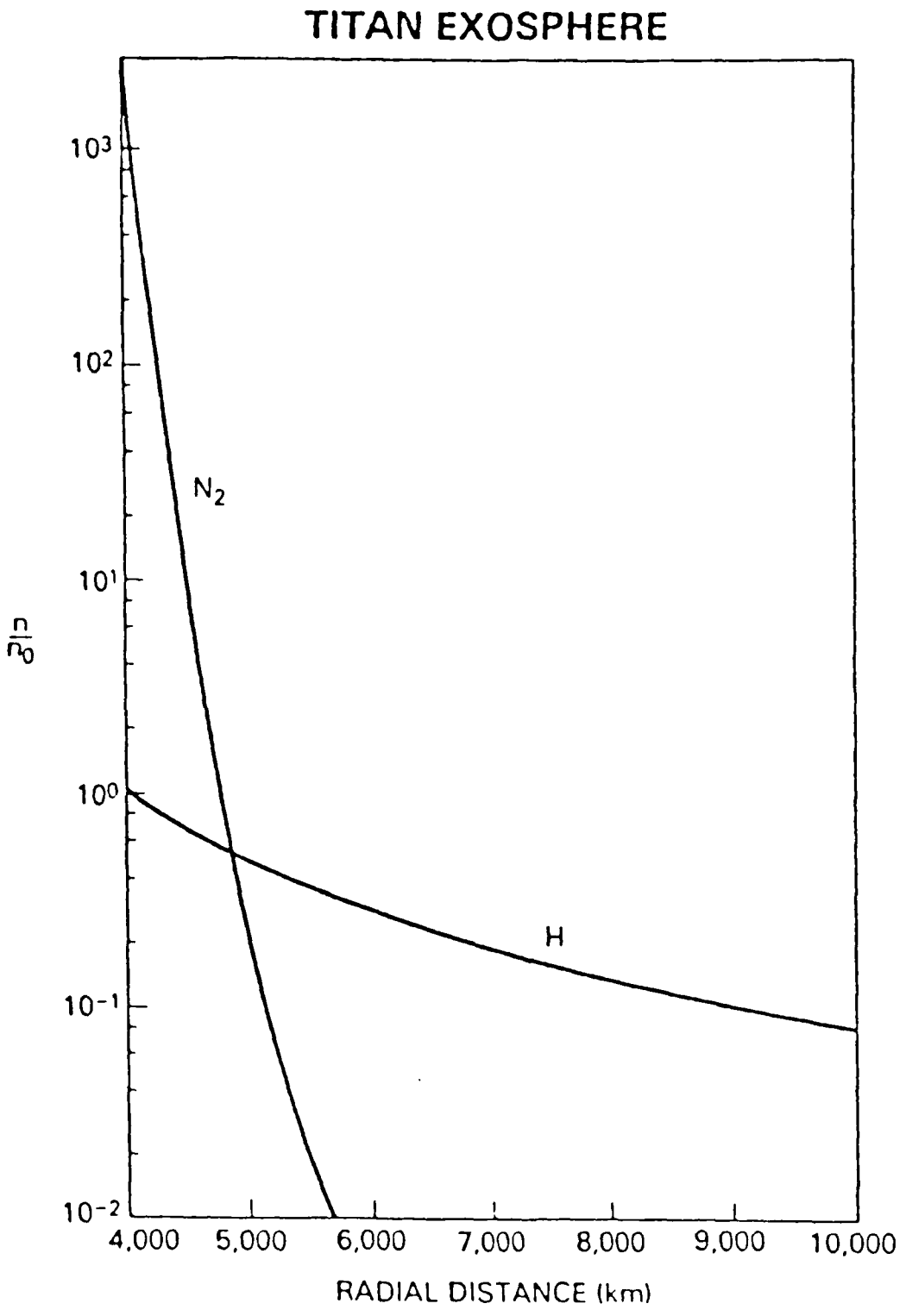
TITAN EXOSPHERE
10^3
10^2
10^1
10^0
10^{-1}
10^{-2}
n/n_0
N_2
H
4,000
5,000
6,000
7,000
8,000
9,000
10,000
RADIAL DISTANCE (km)

Figure 2

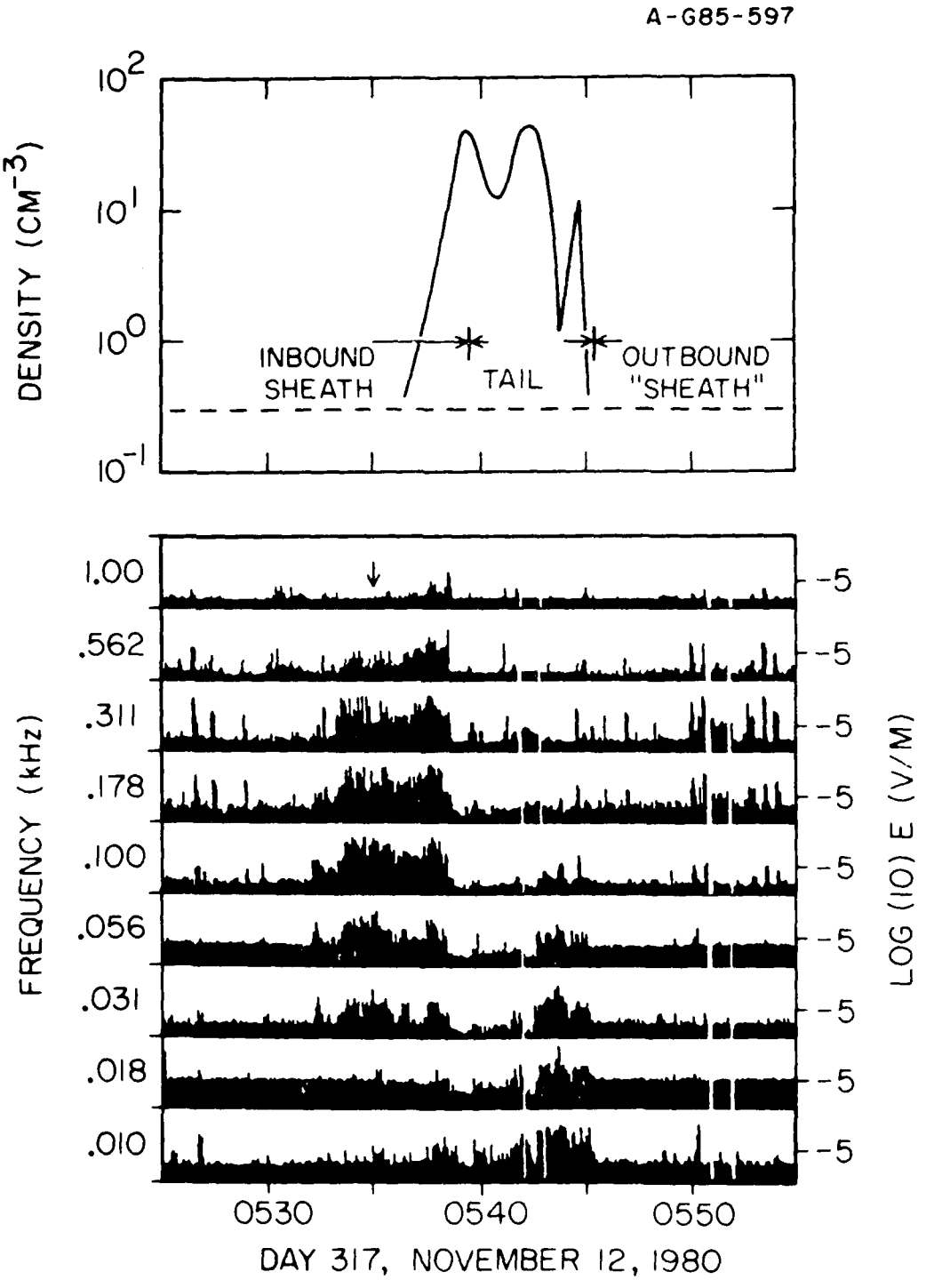
A-G85-597
DENSITY (CM^{-3})
10^2
10^1
10^0
10^{-1}
INBOUND SHEATH
TAIL
OUTBOUND "SHEATH"
FREQUENCY (kHz)
1.00
.562
.311
.178
.100
.056
.031
.018
.010
LOG (10) E (V/M)
-5
0530
0540
0550
DAY 317, NOVEMBER 12, 1980

Figure 3

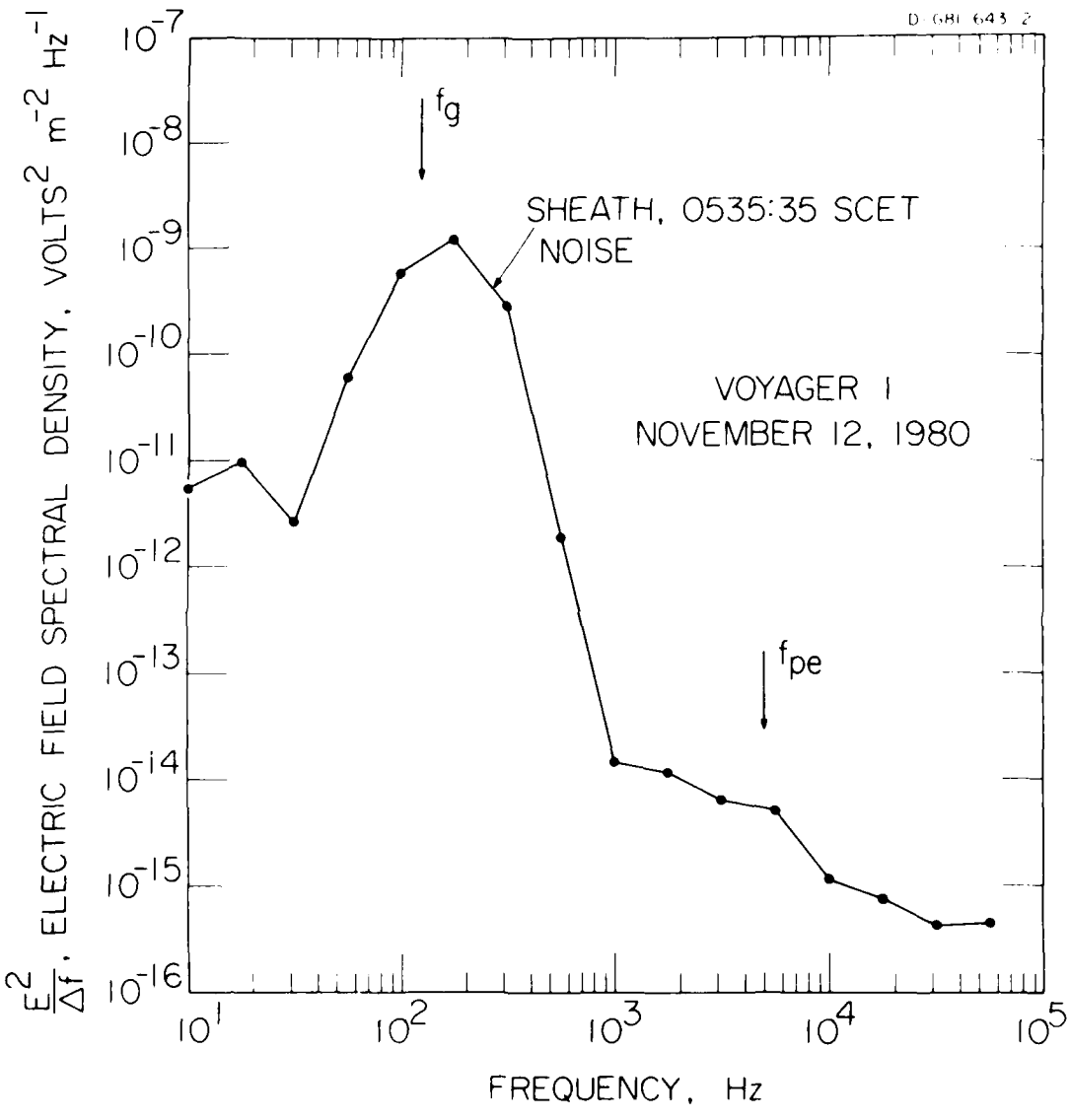
D GBI 643 2
$\frac{E^2}{\Delta f}$, ELECTRIC FIELD SPECTRAL DENSITY, VOLTS^2 m^{-2} Hz^{-1}
10^{-7}
10^{-8}
10^{-9}
10^{-10}
10^{-11}
10^{-12}
10^{-13}
10^{-14}
10^{-15}
10^{-16}
f_g
SHEATH, 0535:35 SCET
NOISE
VOYAGER 1
NOVEMBER 12, 1980
f_{pe}
10^1
10^2
10^3
10^4
10^5
FREQUENCY, Hz

Figure 4

A-G85-516-3

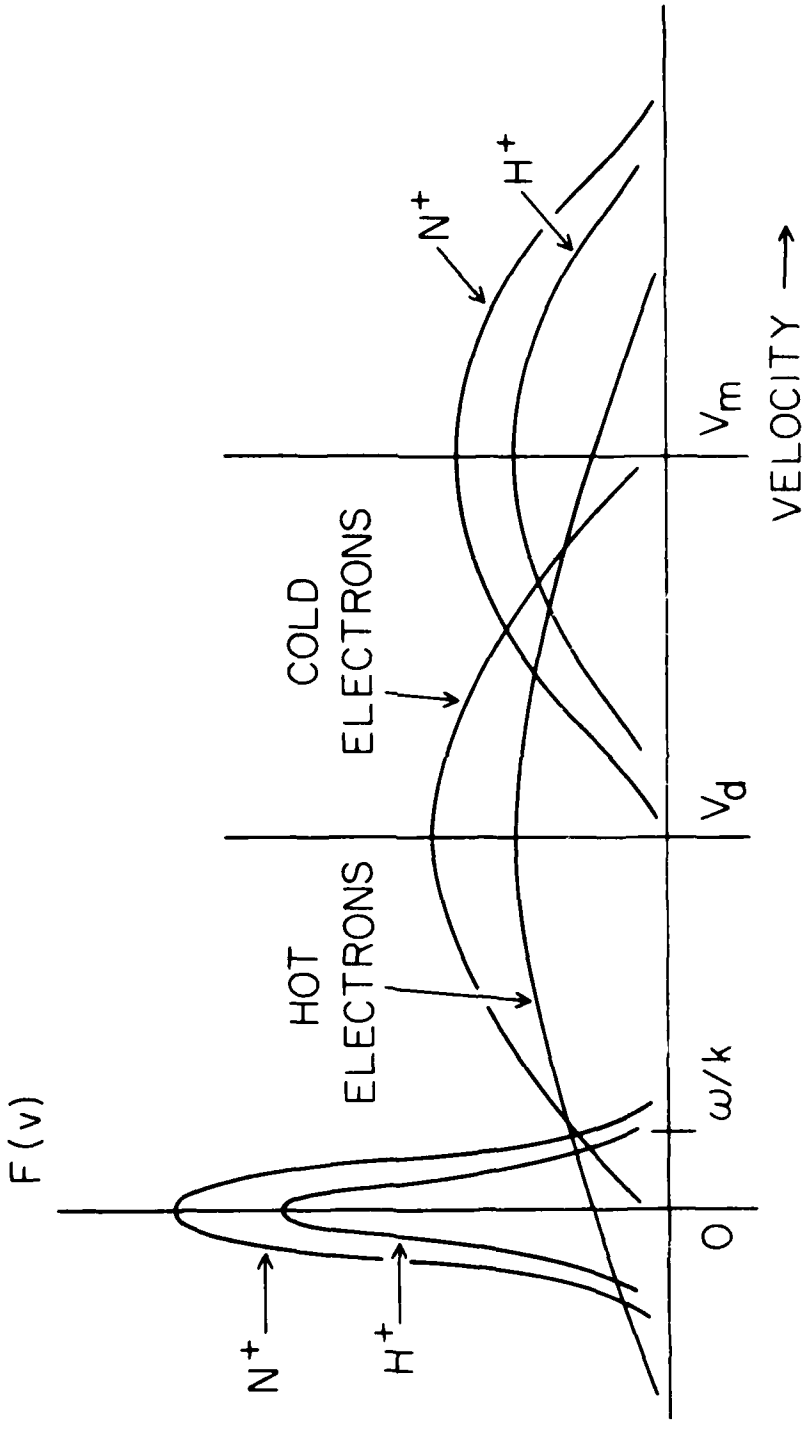

Figure 5

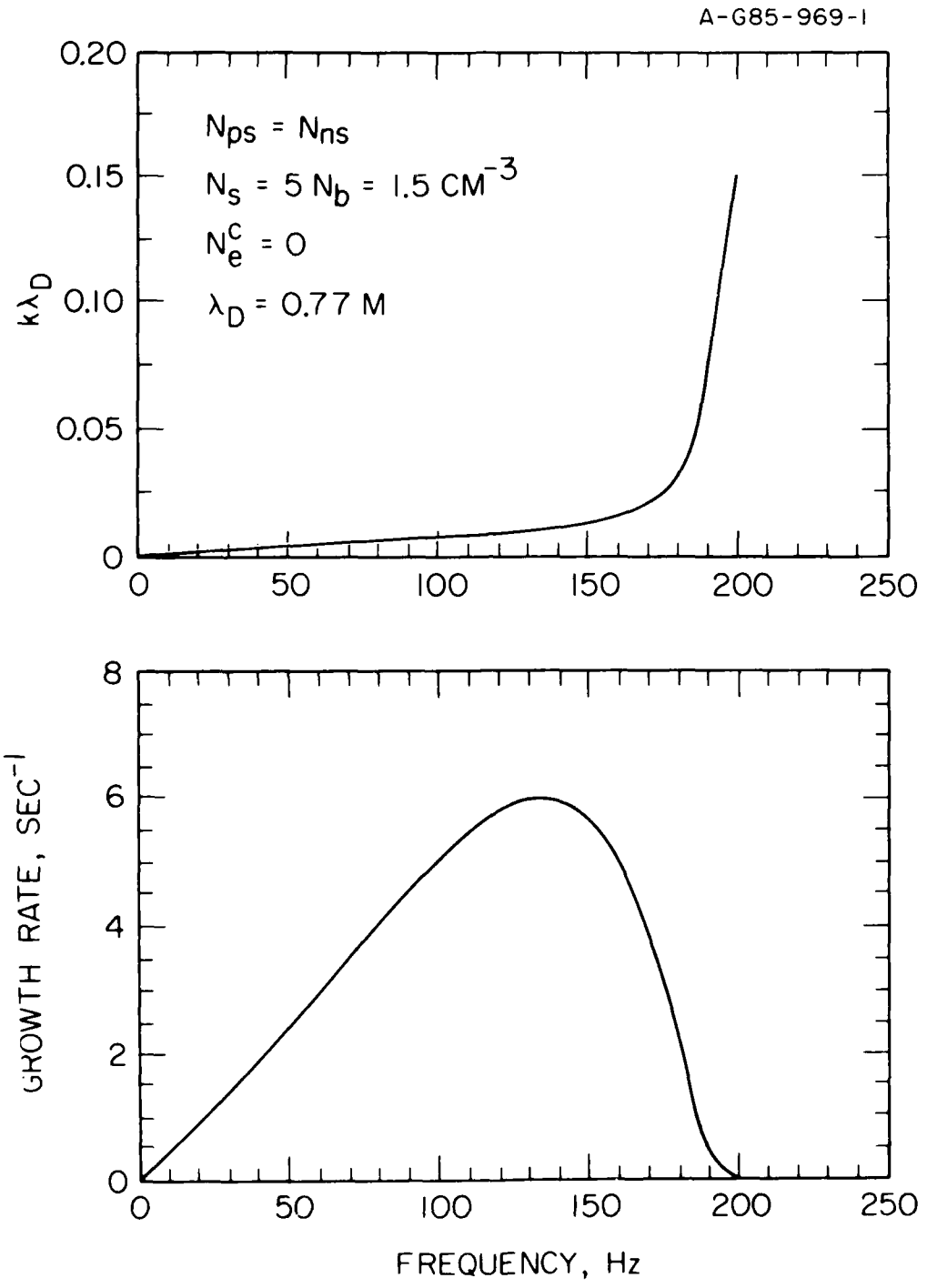
A-G85-969-1
0.20
0.15
0.10
0.05
0
kλD
Nps = Nns
Ns = 5 Nb = 1.5 CM-3
Nec = 0
λD = 0.77 M
0
50
100
150
200
250
8
6
4
2
0
GROWTH RATE, SEC-1
FREQUENCY, Hz

Figure 6

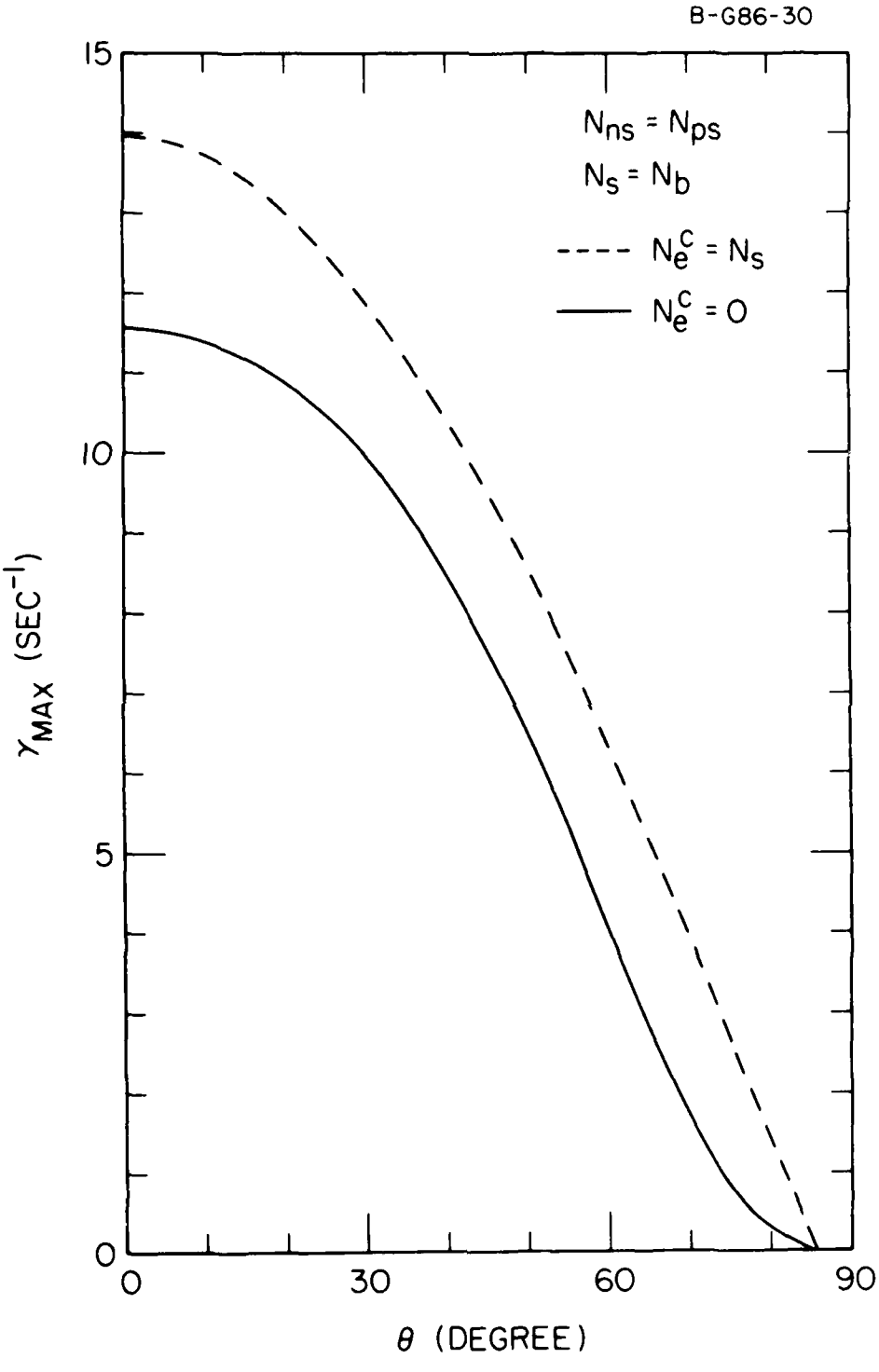
B-G86-30
15
10
5
0
0
30
60
90
γ_{MAX} (SEC^{-1})
θ (DEGREE)
$N_{ns} = N_{ps}$
$N_s = N_b$
$N_e^c = N_s$
$N_e^c = 0$

Figure 7

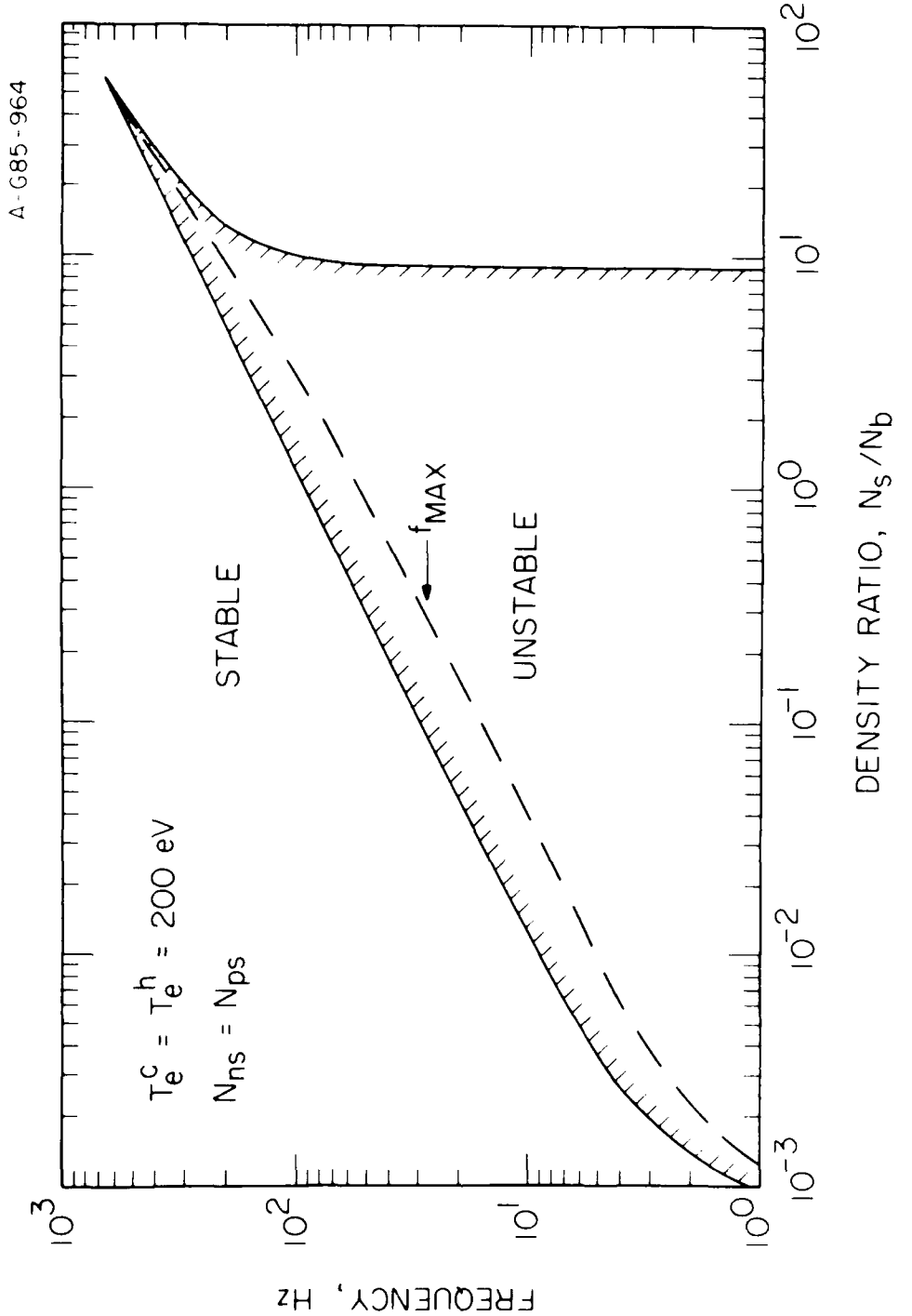
A-G85-964
FREQUENCY, Hz
DENSITY RATIO, N_s/N_b
$T_e^c = T_e^h = 200$ eV
$N_{ns} = N_{ps}$
STABLE
UNSTABLE
f_{MAX}
10^3
10^2
10^1
10^0
10^{-3}
10^{-2}
10^{-1}
10^0
10^1
10^2

Figure 8

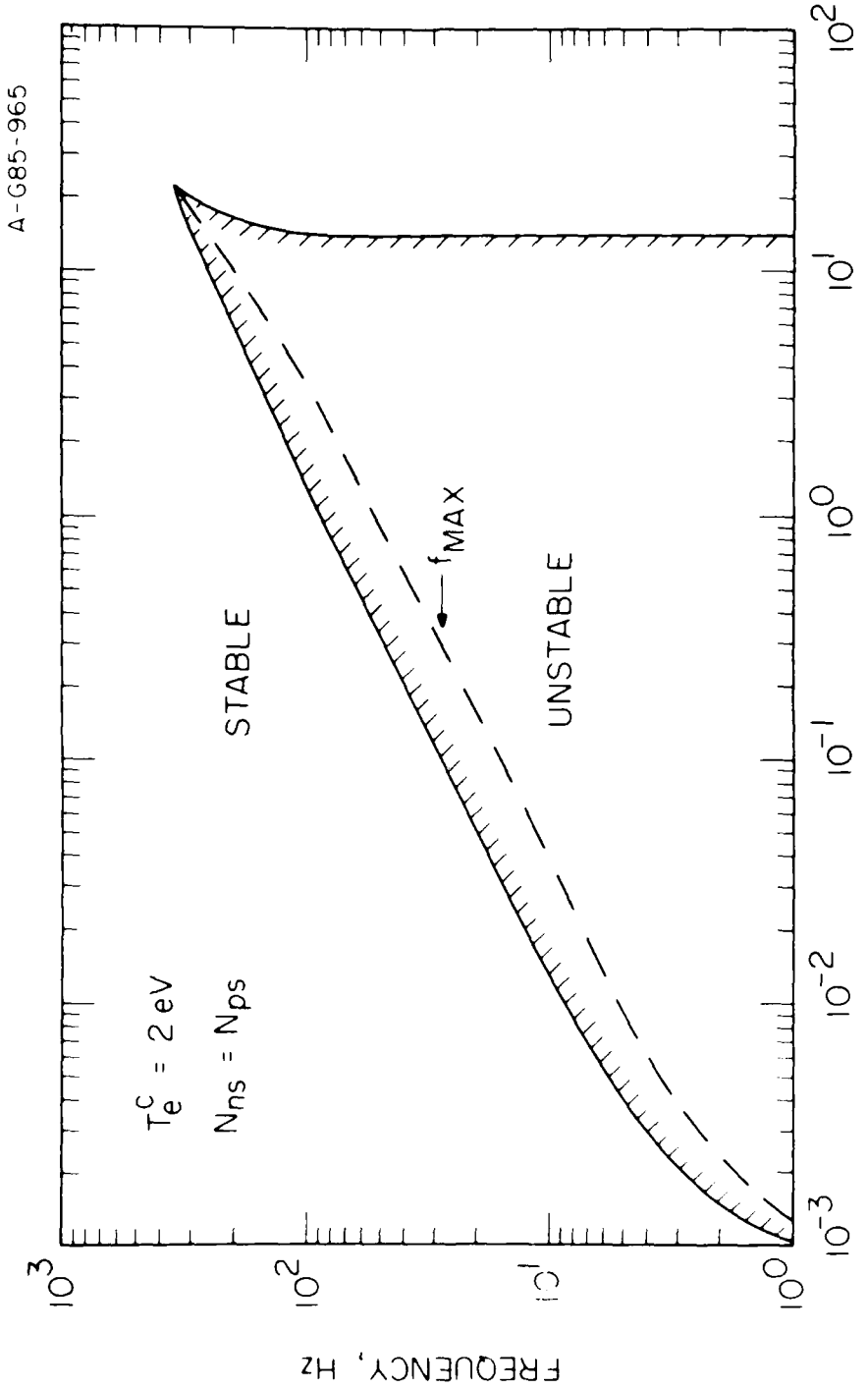
A-G85-965
FREQUENCY, Hz
DENSITY RATIO, N_s/N_b
STABLE
UNSTABLE
f_{MAX}
T_e^c = 2 eV
$N_{ns} = N_{ps}$
10^3
10^2
10^1
10^0
10^{-3}
10^{-2}
10^{-1}
10^0
10^1
10^2

Figure 9

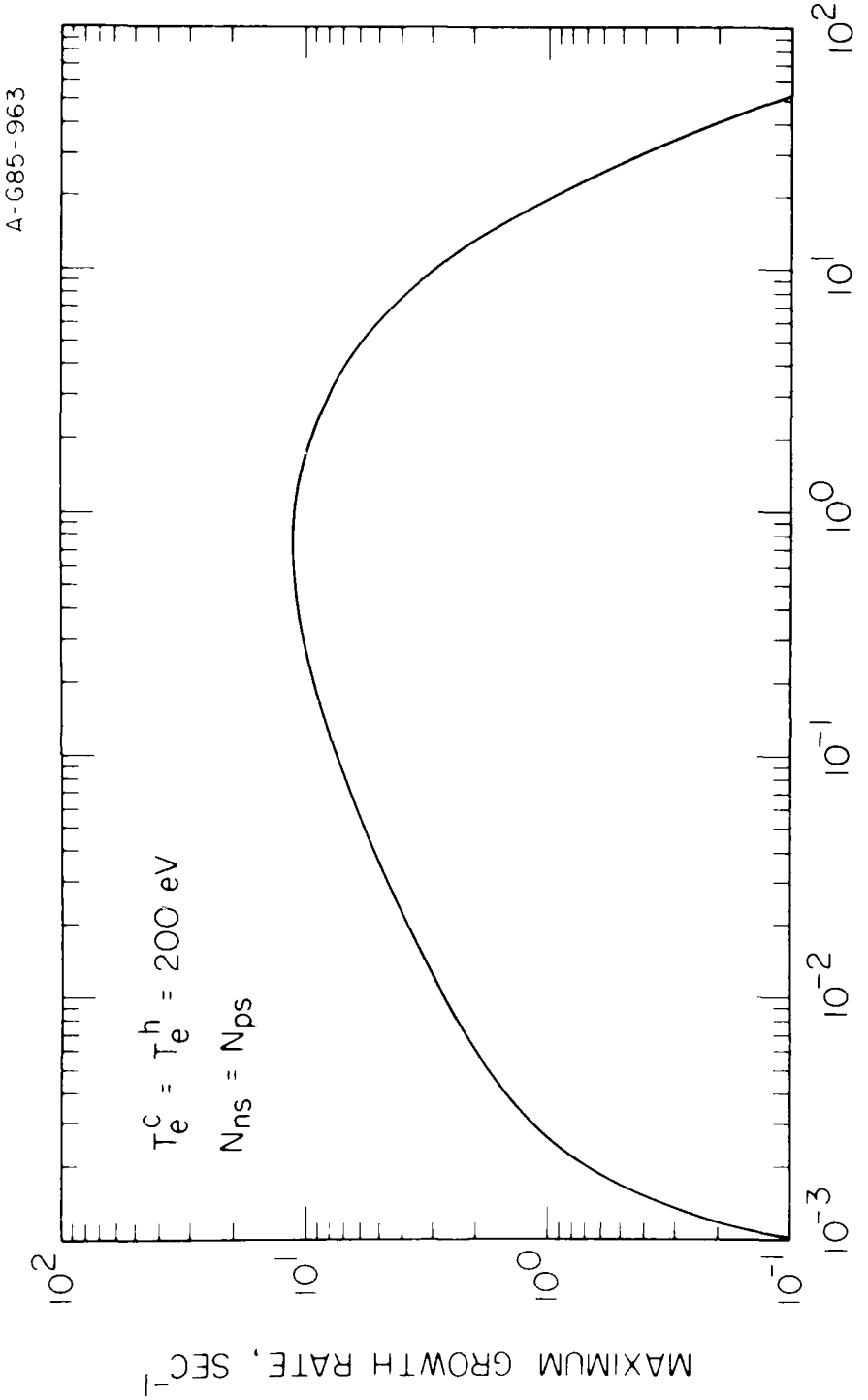
A-G85-963
$T_e^c = T_e^h = 200$ eV
$N_{ns} = N_{ps}$
MAXIMUM GROWTH RATE, SEC^{-1}
DENSITY RATIO, N_s/N_b
10^2
10^1
10^0
10^{-1}
10^{-3}
10^{-2}
10^{-1}
10^0
10^1
10^2

Figure 10

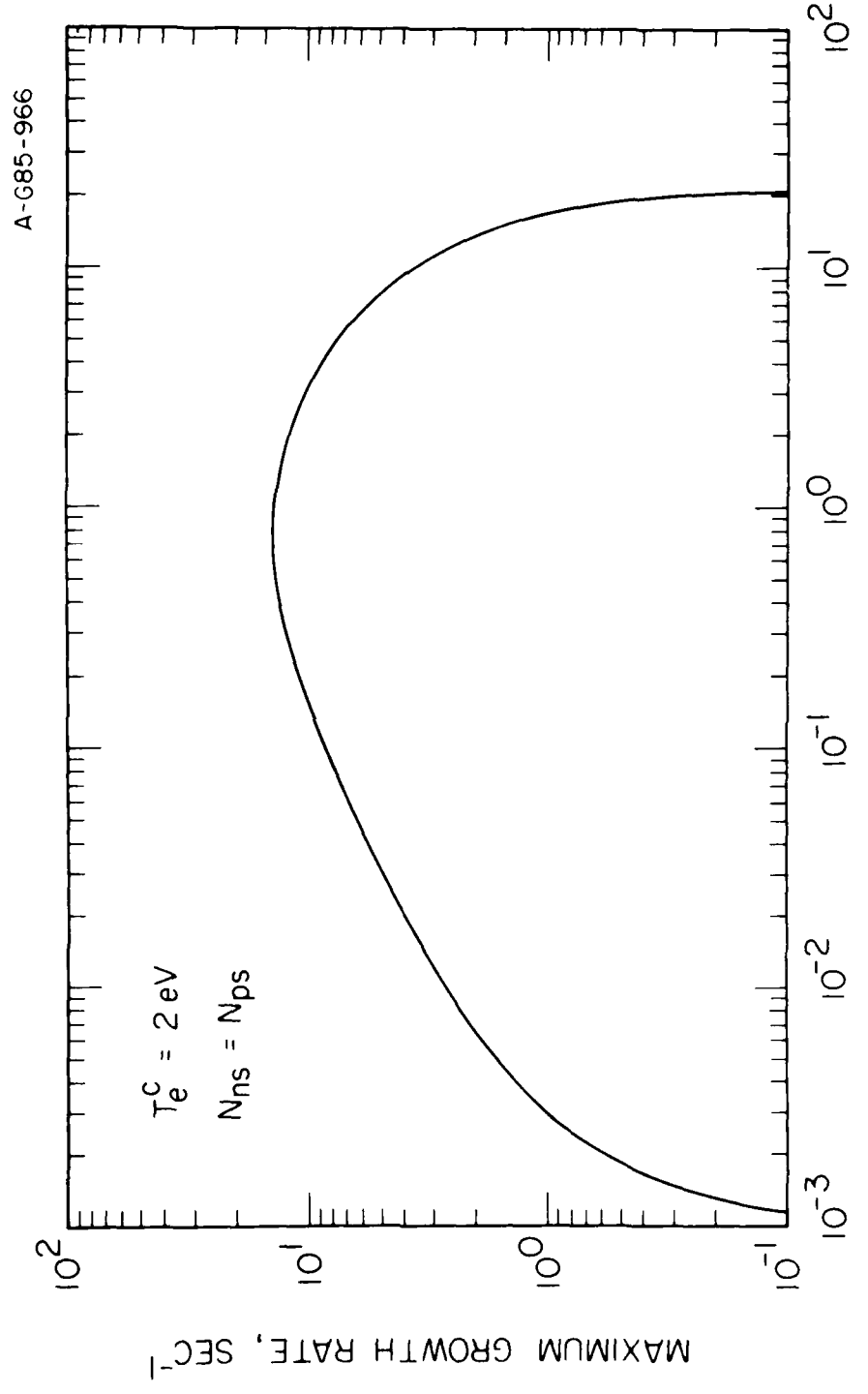
A-685-966
T_e^c = 2 eV
$N_{ns} = N_{ps}$
MAXIMUM GROWTH RATE, SEC^{-1}
DENSITY RATIO, N_s/N_b
10^2
10^1
10^0
10^{-1}
10^{-3}
10^{-2}
10^{-1}
10^0
10^1
10^2

Figure 11

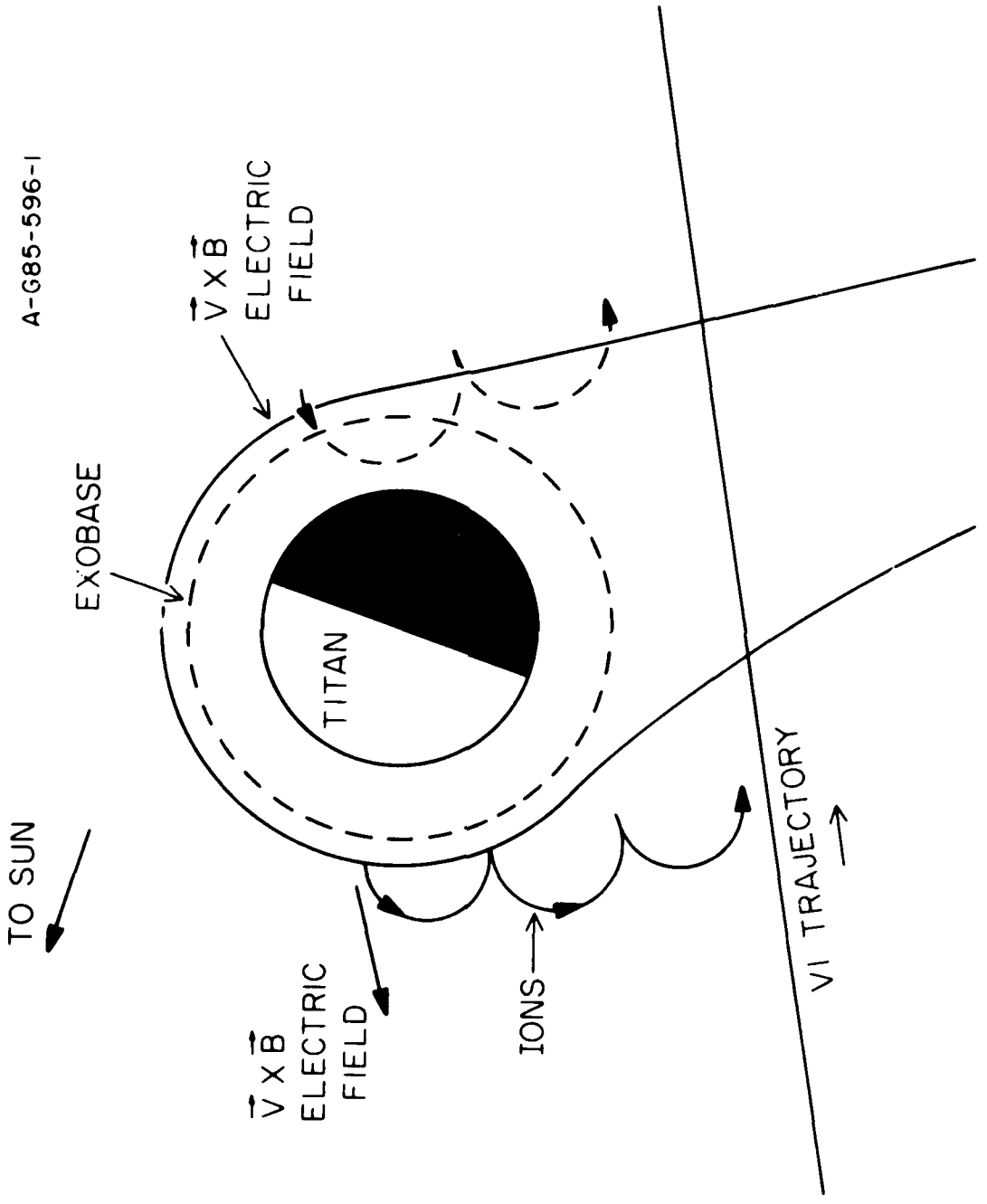
A-G85-596-1
$\vec{V} \times \vec{B}$ ELECTRIC FIELD
EXOBASE
TITAN
TO SUN
$\vec{V} \times \vec{B}$ ELECTRIC FIELD
IONS
VI TRAJECTORY

Figure 12

A-G85-1010

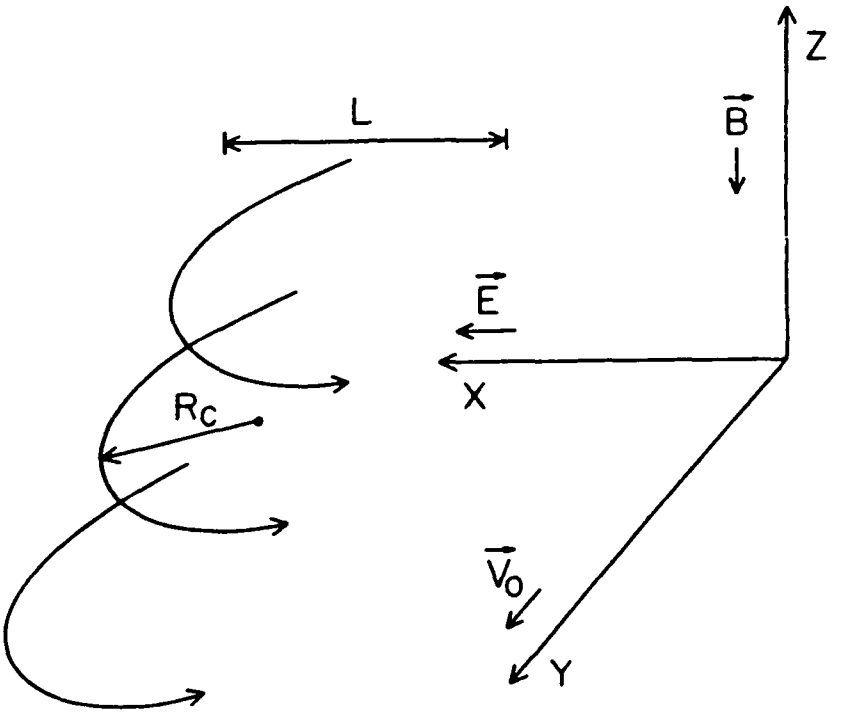

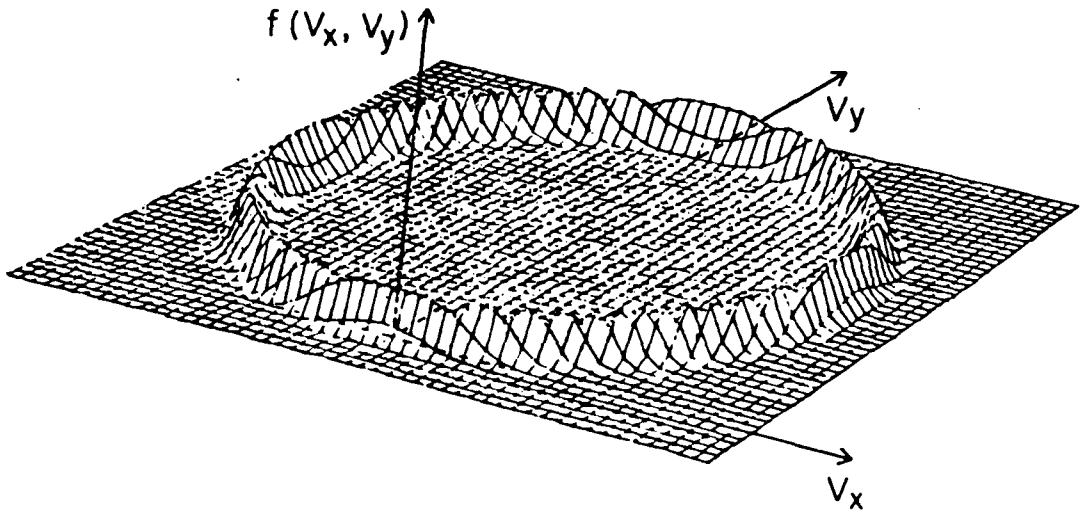

Figure 13

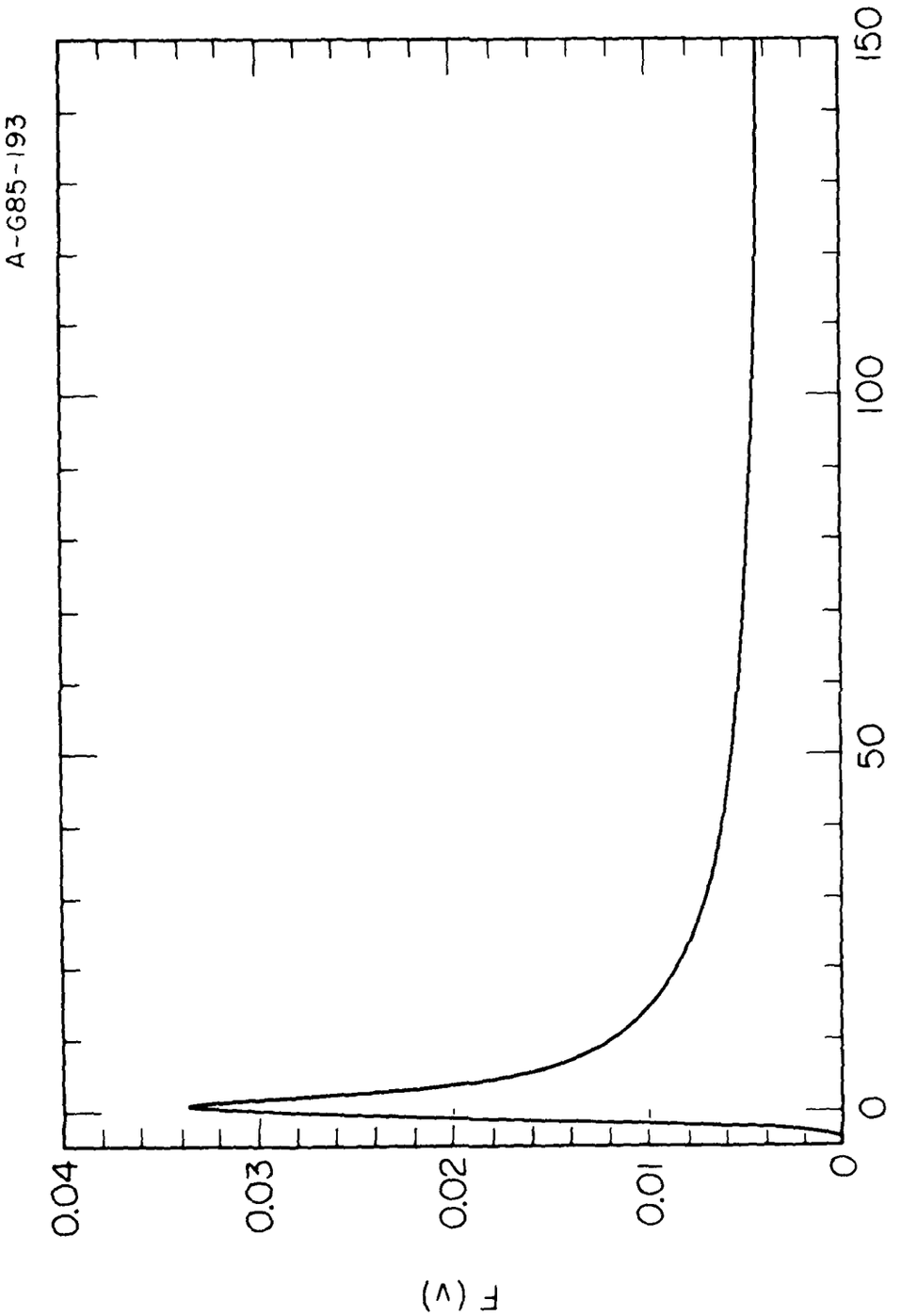

Figure 14

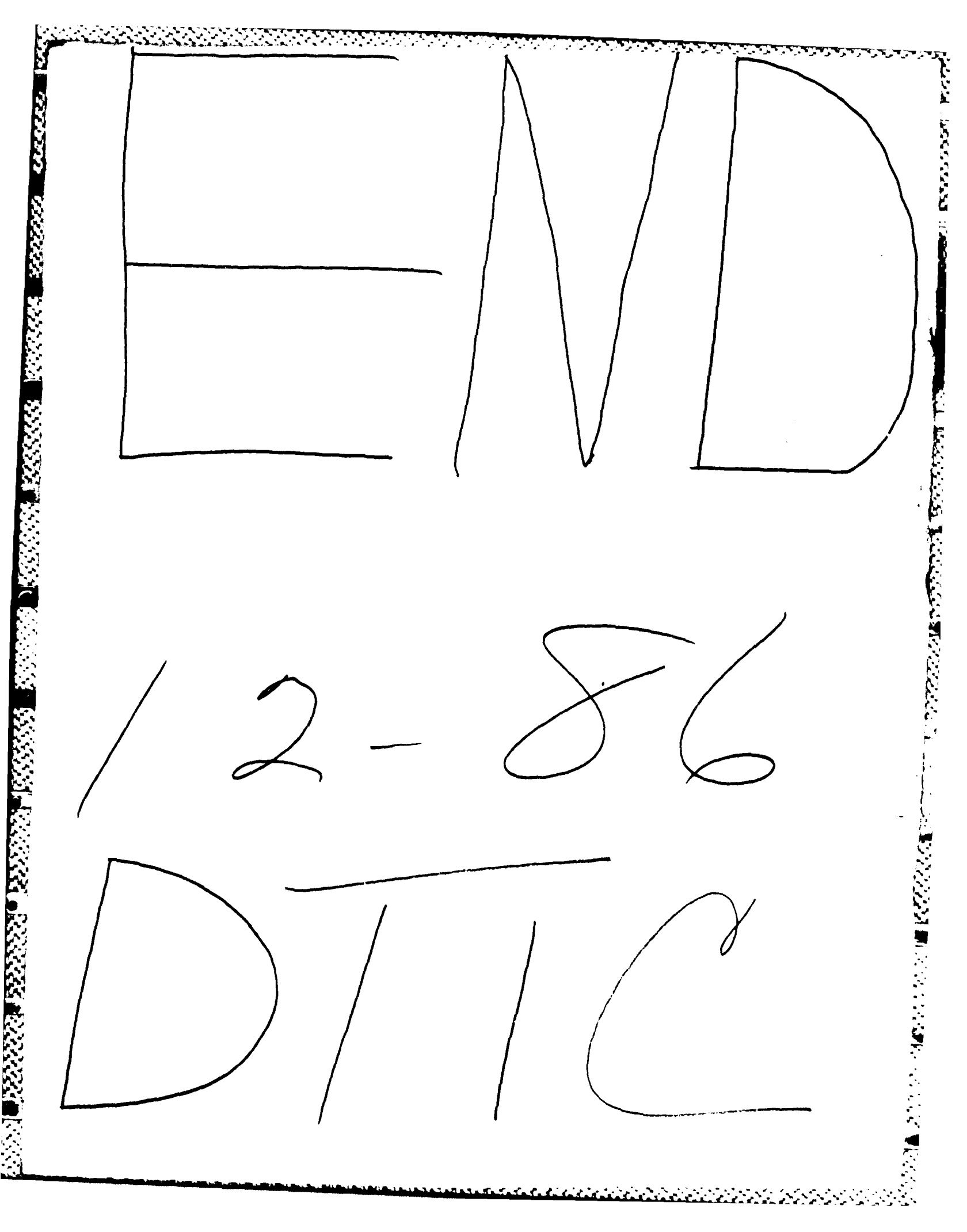
END
12-86
DTIC